

Double Hopf bifurcation of a diffusive predator–prey system with strong Allee effect and two delays*

Yuying Liu^a, Junjie Wei^{a,b} 

^aSchool of Mathematics, Harbin Institute of Technology,
Harbin, Heilongjiang, 150001, China
weijj@hit.edu.cn

^bSchool of Science, Jimei University,
Xiamen, Fujian, 361021, China

Received: October 28, 2019 / **Revised:** March 25, 2020 / **Published online:** January 1, 2021

Abstract. In this paper, we consider a diffusive predator–prey system with strong Allee effect and two delays. First, we explore the stability region of the positive constant steady state by calculating the stability switching curves. Then we derive the Hopf and double Hopf bifurcation theorem via the crossing directions of the stability switching curves. Moreover, we calculate the normal forms near the double Hopf singularities by taking two delays as parameters. We carry out some numerical simulations for illustrating the theoretical results. Both theoretical analysis and numerical simulation show that the system near double Hopf singularity has rich dynamics, including stable spatially homogeneous and inhomogeneous periodic solutions. Finally, we evaluate the influence of two parameters on the existence of double Hopf bifurcation.

Keywords: predator–prey, strong Allee effect, double Hopf bifurcation, two delays, stability switching curves.

1 Introduction

In nature, population growth is limited by environmental resources, this explains why the population cannot grow indefinitely. A proper population growth rate is crucial in describing the population dynamics. The logistic growth proposed by Pearl and Reed in 1920 [18] has been studied by many scholars since then. It assumes that per capita growth rate is a monotonically decreasing function of the population density. The logistic growth considers the intraspecific competition among individuals for limited resources. In ecology, intraspecific competition involves competition for food, mates, shelters, and so on. However, for many social animals, the individual can benefit from the presence of conspecifics, the intraspecific cooperation cannot be ignored. Behaviours of intraspecific cooperation include cooperative predation, cooperative defense against enemies, etc.

*This research was supported by National Natural Science Foundation of China (grant No. 11771109).

The strong Allee effect growth characterizes the population growth of both intraspecific cooperation and intraspecific competition [1, 8, 13], which means the growth rate would be negative when the population density is below a threshold [15, 19]. For the strong Allee effect, the most commonly used expression is

$$f(u) = ru(u - \beta) \left(1 - \frac{u}{K} \right),$$

where $0 < \beta < K$ is the Allee threshold. Obviously, when $u < \beta$, the growth is negative, and the population will eventually die out. This phenomenon is abundant in ecology [4, 13], include inbreeding depression, failure to satiate natural enemies, failure in mate finding, and so on.

In population dynamics, delay occurs in almost every situation, and its effect cannot be neglected [14]. Time delays tend to destabilize the system and lead to oscillatory behavior. Indeed, population densities of many species are known to fluctuate nearly periodically over time [20], a phenomenon to which the delay may provide an explanation. Notice that both the positive feedback of intraspecific cooperation and the negative feedback of intraspecific competition can have delay to the growth of the population. Chang et al. [5] investigated the dynamics of a scalar population model with delayed Allee effect as follows:

$$u'(t) = ru(t)[u(t - \tau) - 1][u(t - \tau) - \theta].$$

They obtained rigorous stability and Hopf bifurcation results for the above model. They showed that the increasing of τ may enlarge the basin of attraction of $u = 0$ and lessen the basin of attraction of $u = 1$. Besides, they showed that large delay may devote to the extinction of the population.

For many species, the delay feedback in intraspecific cooperation is not necessarily the same as that in intraspecific competition. Jankovic and Petrovskii investigated two models as follows [13]:

$$\begin{aligned} \dot{U}(t) &= \gamma U(t)[U(t) - \beta][K - U(t - \tau)], \\ \dot{U}(t) &= \gamma U(t)[U(t - \tau) - \beta][K - U(t)]. \end{aligned}$$

They found that the inclusion of delay in intraspecific cooperation term does not necessarily confer instability, but a delay in intraspecific competition always results in instability, thus leads to population cycles or even extinction. Besides, they obtained that delay in competition term has more dominant effects on population dynamics compared to the delay in cooperation term.

Besides, the digestion or gestation delay plays an important role in characterizing the increase of the predator growth. Recently, many researchers consider the digestion delay in their models [3, 6, 7, 17, 23]. Chen et al. [6] proposed a diffusive predator–prey model with digestion delay. They investigated the effect of the digestion delay on the system and obtained the stability of the equilibria and the existence of Hopf bifurcation.

Motivated by the previous works, we introduce a delay in intraspecific competition in prey, consider the digestion delay in predator, and conclude a diffusive predator–prey

system with strong Allee effect with two delays as follows:

$$\begin{aligned} \frac{\partial u}{\partial t} &= d_1 \Delta u + ru(u - c) \left(1 - \frac{u(t - \tau_1)}{K} \right) - \frac{muv}{b + u}, \quad x \in \Omega, t > 0, \\ \frac{\partial v}{\partial t} &= d_2 \Delta v + \frac{mu(t - \tau_2)v}{b + u(t - \tau_2)} - dv, \quad x \in \Omega, t > 0, \\ \partial_\nu u &= \partial_\nu v = 0, \quad x \in \partial\Omega, t > 0, \end{aligned} \quad (1)$$

where $u = u(x, t)$, $v = v(x, t)$ denote the density of the prey and predator at location x and time t , respectively; d_1 , d_2 mean the diffusion coefficients; τ_1 , τ_2 denote the delay feedback of intraspecific competition in prey and the digestion delay in predator, respectively; c denotes the Allee threshold, and K is the carrying capacity; m represents the modified capture rate; b denotes the semi-saturation coefficient, and d the death rate of predator. The homogeneous Neumann boundary condition is imposed so that there is no population flow across the boundary, ν denotes the outward normal to the boundary $\partial\Omega$. For simplicity, we choose Ω as a spatial interval $[0, l\pi]$.

Our purpose is to explore the joint effect of two delays on the dynamics of system (1). The introduction of one delay may destabilize the equilibria, lead to the occurrence of Hopf bifurcation [24]. The dynamics of the system with two delays would be more complex. There are several related studies on systems with two delays [2, 21, 22]. Most of the works regard one delay as a constant and the other as variable. To evaluate the joint effect of two delays, it is necessary to take two delays as variables. Gu et al. [11] and Wang et al. [16] provide methods in studying the stability of a system with two delays vary simultaneously. Du et al. investigated a diffusive Leslie–Gower model with two delays [10], they performed the stability analysis and explored the existence of double Hopf bifurcation.

The highlights of this paper are as follows. For one thing, the Hopf bifurcation curves and double Hopf bifurcation curves on a two-parameter plane are given. For another, the calculation of the normal forms near the double Hopf singularity need subtle analysis, since two simultaneously varying delays make the calculation process more complex. Besides, the stable spatially homogeneous and inhomogeneous periodic solutions are theoretically proved and illustrated near the double Hopf singularities.

Our paper is organized as follows. In Section 2, we obtain the stability switching curves of the positive equilibrium and present the Hopf and double Hopf bifurcation theorem. In Section 3, we calculate the normal forms on the center manifold near the double Hopf singularity. In Section 4, we carry out some numerical simulations for illustrating the theoretical results. Finally, conclusions are made to sum up the paper.

2 Stability switching curves and the existence of double Hopf bifurcation

In this section, we perform the stability and bifurcation analysis of the system.

2.1 Stability switching curves

By direct calculation, system (1) has three constant steady states $E_0(0, 0)$, $E_1(c, 0)$, $E_2(K, 0)$ and a possible positive constant steady state $E_*(u_*, v_*)$, where $u_* = bd/(m-d)$, $v_* = r(u_* - c)(u_* + b)(1 - u_*/K)/m$. To guarantee the existence of E_* , we make the following assumption:

$$(H0) \quad c < bd/(m - d) < K.$$

Since the study of boundary equilibria is of little biological significance, in this paper, we focus on the study of E_* and assume that (H0) is always true.

The linearization of system (1) at E_* is

$$\frac{\partial}{\partial t} \begin{pmatrix} u(x, t) \\ v(x, t) \end{pmatrix} = (D\Delta + A) \begin{pmatrix} u(x, t) \\ v(x, t) \end{pmatrix} + B \begin{pmatrix} u(x, t - \tau_1) \\ v(x, t - \tau_1) \end{pmatrix} + C \begin{pmatrix} u(x, t - \tau_2) \\ v(x, t - \tau_2) \end{pmatrix},$$

where

$$D = \begin{pmatrix} d_1 & 0 \\ 0 & d_2 \end{pmatrix}, \quad A = \begin{pmatrix} ru_*(1 - \frac{u_*}{K})(\frac{2u_* + b - c}{b + u_*}) & -d \\ 0 & 0 \end{pmatrix},$$

$$B = \begin{pmatrix} -\frac{r}{K}u_*(u_* - c) & 0 \\ 0 & 0 \end{pmatrix}, \quad C = \begin{pmatrix} 0 & 0 \\ \frac{mbv_*}{(b + u_*)^2} & 0 \end{pmatrix}.$$

Then the characteristic equation of E_* is

$$\det(\lambda I_2 - M_n - A - Be^{-\lambda\tau_1} - Ce^{-\lambda\tau_2}) = 0, \tag{2}$$

where I_2 is the 2×2 identity matrix, and $M_n = -(n^2/l^2)D$. For simplicity, denote

$$a_{11} = ru_* \left(1 - \frac{u_*}{K}\right) \left(\frac{2u_* + b - c}{b + u_*}\right),$$

$$b_{11} = -\frac{r}{K}u_*(u_* - c), \quad c_{21} = \frac{mbv_*}{(b + u_*)^2}.$$

Then (2) is equivalent to

$$D_n(\lambda; \tau_1, \tau_2) := P_{0,n}(\lambda) + P_{1,n}(\lambda)e^{-\lambda\tau_1} + P_{2,n}(\lambda)e^{-\lambda\tau_2} = 0, \quad n \in \mathbb{N}_0, \tag{3}$$

where

$$P_{0,n}(\lambda) = \left(\lambda + d_1 \frac{n^2}{l^2} - a_{11}\right) \left(\lambda + d_2 \frac{n^2}{l^2}\right), \tag{4}$$

$$P_{1,n}(\lambda) = -b_{11} \left(\lambda + d_2 \frac{n^2}{l^2}\right), \quad P_{2,n}(\lambda) = dc_{21}.$$

To maintain the stability of E_* at $\tau_1 = \tau_2 = 0$, we further make the hypothesis

$$(H1) \quad (K - u_*)(2u_* + b - c)/(b + u_*) < u_* - c.$$

Then we can easily get the following theorem.

Theorem 1. *If (H0) and (H1) hold, E_* is locally asymptotically stable for $\tau_1 = \tau_2 = 0$.*

Now we will investigate the joint effect of τ_1 and τ_2 on the stability of E_* under (H0) and (H1). To apply the method of the stability switching curves, we first check assumptions (I)–(IV) in [16] for all $n \in \mathbb{N}_0$. Obviously, (I)–(IV) are true for $P_{0,n}(\lambda)$, $P_{1,n}(\lambda)$ and $P_{2,n}(\lambda)$ in Eq. (4). Particularly, assumption (IV) maintains feasible ω 's to be bounded.

To proceed the analysis, we introduce the following lemma [21].

Lemma 1. *As (τ_1, τ_2) varies continuously in \mathbb{R}_+^2 , the number of zeros (with multiplicity counted) of $D_n(\lambda; \tau_1, \tau_2)$ on \mathbb{C}_+ can change only if a zero appears or cross the imaginary axis.*

Since $\lambda = 0$ is not a zero of (3), we will seek purely imaginary zeros of (3) to explore the stability switching curves. Assume $\lambda = i\omega$ ($\omega > 0$) is a zero of (3), then

$$P_{0,n}(i\omega) + P_{1,n}(i\omega)e^{-i\omega\tau_1} = -P_{2,n}(i\omega)e^{-i\omega\tau_2}.$$

Since $|e^{-i\omega\tau_2}| = 1$, after simplification, we obtain

$$\begin{aligned} &|P_{0,n}(i\omega)|^2 + |P_{1,n}(i\omega)|^2 - |P_{2,n}(i\omega)|^2 \\ &= 2[A_{1,n}(\omega) \cos(\omega\tau_1) - B_{1,n}(\omega) \sin(\omega\tau_1)], \end{aligned} \tag{5}$$

where $A_{1,n}(\omega) = \text{Re}(-P_{0,n}(i\omega)\overline{P_{1,n}(i\omega)})$, $B_{1,n}(\omega) = \text{Im}(-P_{0,n}(i\omega)\overline{P_{1,n}(i\omega)})$.

Without loss of generality, assume $A_{1,n}^2(\omega) + B_{1,n}^2(\omega) > 0$, then there exists some continuous function $\phi_{1,n}(\omega) \in \text{Arg}\{-P_{0,n}(i\omega)\overline{P_{1,n}(i\omega)}\} \cap (-\pi, 2\pi]$ such that (5) becomes

$$\begin{aligned} &|P_{0,n}(i\omega)|^2 + |P_{1,n}(i\omega)|^2 - |P_{2,n}(i\omega)|^2 \\ &= 2\sqrt{A_{1,n}^2(\omega) + B_{1,n}^2(\omega)} \cos(\omega\tau_1 + \phi_{1,n}(\omega)), \end{aligned} \tag{6}$$

then the existence of $\tau_1 \in \mathbb{R}_+$ in (6) equals

$$||P_{0,n}(i\omega)|^2 + |P_{1,n}(i\omega)|^2 - |P_{2,n}(i\omega)|^2| \leq 2\sqrt{A_{1,n}^2(\omega) + B_{1,n}^2(\omega)}. \tag{7}$$

Obviously, Eq. (7) contains the special case $A_1^2(\omega) + B_1^2(\omega) = 0$. We denote Ω_n^1 to be the collection of positive ω 's such that (7) hold. Let $\psi_{1,n}(\omega) \in [0, \pi]$ satisfies

$$\begin{aligned} \cos(\psi_{1,n}(\omega)) &= \cos(\omega\tau_1 + \phi_{1,n}(\omega)) \\ &= \frac{|P_{0,n}(i\omega)|^2 + |P_{1,n}(i\omega)|^2 - |P_{2,n}(i\omega)|^2}{2\sqrt{A_{1,n}^2(\omega) + B_{1,n}^2(\omega)}}, \end{aligned}$$

then we have

$$\tau_{1,j_1,n}^\pm = \frac{\pm\psi_{1,n}(\omega) - \phi_{1,n}(\omega) + 2j_1\pi}{\omega}, \quad j_1 \in \mathbb{Z}. \tag{8}$$

Similarly, we can get that

$$\begin{aligned} \tau_{2,j_2,n}^\pm &= \frac{\pm\psi_{2,n}(\omega) - \phi_{2,n}(\omega) + 2j_2\pi}{\omega}, \quad j_2 \in \mathbb{Z}, \\ \cos(\psi_{2,n}(\omega)) &= \frac{|P_{0,n}(i\omega)|^2 - |P_{1,n}(i\omega)|^2 + |P_{2,n}(i\omega)|^2}{2\sqrt{A_{2n}^2(\omega) + B_{2n}^2(\omega)}}, \\ A_{2,n}(\omega) &= \operatorname{Re}(-P_{0,n}(i\omega)\overline{P_{2,n}(i\omega)}), \quad B_{2,n}(\omega) = \operatorname{Im}(-P_{0,n}(i\omega)\overline{P_{2,n}(i\omega)}), \\ \phi_{2,n}(\omega) &\in \operatorname{Arg}\{-P_{0,n}(i\omega)\overline{P_{2,n}(i\omega)}\} \cap (-\pi, 2\pi], \end{aligned} \tag{9}$$

where ω satisfies the following condition:

$$\left| |P_{0,n}(i\omega)|^2 - |P_{1,n}(i\omega)|^2 + |P_{2,n}(i\omega)|^2 \right| \leq 2\sqrt{A_{2,n}(\omega)^2 + B_{2,n}(\omega)^2}. \tag{10}$$

Denote Ω_n^2 as the collection of all ω 's such that (10) hold, by squaring both side of (7) and (10), we can get that $\Omega_n^1 = \Omega_n^2$. For simplicity, denote $\Omega_n := \Omega_n^1 = \Omega_n^2$.

To clarify that the stability switching curves of a finite region contains all the stability switching curves in that region, we present the following lemma.

Lemma 2. Ω_n consists of a finite number of intervals of finite length.

The above lemma can be easily proved, here we omit the proof.

In the following, we will investigate the relationship between different stability switching curves. From Eqs. (8) and (9), for any $\omega \in \Omega_n$, on the corresponding stability switching curves, one can obtain either $\tau_{2,j_2,n}^+$ or $\tau_{2,j_2,n}^-$ for a given $\tau_{1,j_1,n}^+$. With the aid of MATLAB, we verify that when $\tau_1 = \tau_{1,j_1,n}^+$, $\tau_2 = \tau_{2,j_2,n}^-$; similarly, when $\tau_1 = \tau_{1,j_1,n}^-$, $\tau_2 = \tau_{2,j_2,n}^+$. Therefore,

$$\begin{aligned} \mathcal{T}_{j_1,j_2,n}^{\pm k} &= \left\{ (\tau_1^\pm(\omega), \tau_2^\mp(\omega)), \omega \in \Omega_{k,n} \right\} \\ &= \left\{ \left(\frac{\pm\psi_{1,n}(\omega) - \phi_{1,n}(\omega) + 2j_1\pi}{\omega}, \frac{\mp\psi_{2,n}(\omega) - \phi_{2,n}(\omega) + 2j_2\pi}{\omega} \right), \omega \in \Omega_{k,n} \right\}, \end{aligned}$$

and

$$\mathcal{T}_n = \bigcup_{j_1, j_2 \in \mathbb{Z}} \bigcup_{k=1,2,\dots,r_n} (\mathcal{T}_{j_1,j_2,n}^{\pm k} \cap \mathbb{R}_+^2).$$

Proposition 1. \mathcal{T}_n is the set of all stability crossing curves on τ_1, τ_2 -plane for $D_n(\lambda; \tau_1, \tau_2) = 0$. For any $(\tau_1, \tau_2) \in \mathcal{T}_n$, $D_n(\lambda; \tau_1, \tau_2) = 0$ has at least one root $i\omega$ with $\omega \in \Omega_n$.

Notice that $F_n(a_{k,n}) = F_n(b_{k,n}) = 0$, then $\psi_{i,n}(a_{k,n}) = \delta_i^{a_{k,n}} \pi$, $\psi_{i,n}(b_{k,n}) = \delta_i^{b_{k,n}} \pi$, where $\delta_i^{a_{k,n}}, \delta_i^{b_{k,n}} = 0, 1$ ($i = 1, 2$). By direct calculation, we can get that

$$\begin{aligned} (\tau_{1,j_1,n}^{+k}(a_{k,n}), \tau_{2,j_2,n}^{-k}(a_{k,n})) &= (\tau_{1,(j_1+\delta_1^a),n}^{-k}(a_{k,n}), \tau_{2,(j_2-\delta_2^a),n}^{+k}(a_{k,n})), \\ (\tau_{1,j_1,n}^{+k}(b_{k,n}), \tau_{2,j_2,n}^{-k}(b_{k,n})) &= (\tau_{1,(j_1+\delta_1^b),n}^{-k}(b_{k,n}), \tau_{2,(j_2-\delta_2^b),n}^{+k}(b_{k,n})). \end{aligned} \tag{11}$$

Obviously, (11) means $\mathcal{T}_{j_1, j_2, n}^{+k}$ connects with $\mathcal{T}_{j_1 + \delta_1^a, j_2 - \delta_2^a, n}^{-k}$ and $\mathcal{T}_{j_1 + \delta_1^b, j_2 - \delta_2^b, n}^{-k}$ at its two ends. In (11), we denote δ_i^a, δ_i^b instead of $\delta_i^{a, n}, \delta_i^{b, n}$, one should in mind that the values of $\delta_i^{a, n}$ or $\delta_i^{b, n}$ might be different for different k, n and i .

2.2 Crossing directions

To present the Hopf bifurcation and double Hopf bifurcation theorem, we define the crossing directions of the points on the stability switching curves in this subsection.

Let $\lambda = \sigma + i\omega$. By the implicit function theorem, τ_1, τ_2 can be expressed as functions of σ and ω under some non-singular condition. For convenience, denote

$$R_0 := \frac{\operatorname{Re}(\partial D(\lambda; \tau_1, \tau_2))}{\partial \sigma} \Big|_{\lambda=i\omega}, \quad I_0 := \frac{\operatorname{Im}(\partial D(\lambda; \tau_1, \tau_2))}{\partial \sigma} \Big|_{\lambda=i\omega},$$

and for $l = 1$ and 2 ,

$$R_l := \frac{\operatorname{Re}(\partial D(\lambda; \tau_1, \tau_2))}{\partial \tau_l} \Big|_{\lambda=i\omega}, \quad I_l := \frac{\operatorname{Im}(\partial D(\lambda; \tau_1, \tau_2))}{\partial \tau_l} \Big|_{\lambda=i\omega}.$$

We can easily verify that

$$\frac{\operatorname{Re}(\partial D(\lambda; \tau_1, \tau_2))}{\partial \omega} \Big|_{\lambda=i\omega} = -I_0, \quad \frac{\operatorname{Im}(\partial D(\lambda; \tau_1, \tau_2))}{\partial \omega} \Big|_{\lambda=i\omega} = R_0.$$

Since $\mathcal{T}_{j_1, j_2, n}^{\pm k}$ are piecewise differentiable, by the implicit function theory, we have

$$\Delta(\omega) := \begin{pmatrix} \frac{\partial \tau_1}{\partial \sigma} & \frac{\partial \tau_1}{\partial \omega} \\ \frac{\partial \tau_2}{\partial \sigma} & \frac{\partial \tau_2}{\partial \omega} \end{pmatrix}_{\substack{\sigma=0 \\ \omega \in \Omega_{n, k}}} = \begin{pmatrix} R_1 & R_2 \\ I_1 & I_2 \end{pmatrix}^{-1} \begin{pmatrix} R_0 & -I_0 \\ I_0 & R_0 \end{pmatrix}$$

as long as the nonsingular condition $R_1 I_2 - R_2 I_1 \neq 0$ holds.

For any crossing curve $\mathcal{T}_{j_1, j_2, n}^{\pm k}$, we define the direction of the curve corresponding to the increasing $\omega \in \Omega_{n, k}$ the *positive direction*. The region on the left-hand (right-hand) side when we move in the positive direction of the curve the *region on the left (right)*. By direct calculation, we get that the tangent vector of $\mathcal{T}_{j_1, j_2, n}^{\pm k}$ along the positive direction is $(\partial \tau_1 / \partial \omega, \partial \tau_2 / \partial \omega)$, the normal vector of $\mathcal{T}_{j_1, j_2, n}^{\pm k}$ pointing to the right region is $(\partial \tau_2 / \partial \omega, -\partial \tau_1 / \partial \omega)$. Besides, a pair of complex characteristic roots across the imaginary axis from the left to the right of the complex plane as σ increases from negative to positive, thus (τ_1, τ_2) moves along $(\partial \tau_1 / \partial \sigma, \partial \tau_2 / \partial \sigma)$. We can deduce that if

$$\delta(\omega) := \begin{pmatrix} \frac{\partial \tau_1}{\partial \sigma} & \frac{\partial \tau_2}{\partial \sigma} \end{pmatrix} \cdot \begin{pmatrix} \frac{\partial \tau_2}{\partial \omega} & -\frac{\partial \tau_1}{\partial \omega} \end{pmatrix} = \frac{\partial \tau_1}{\partial \sigma} \frac{\partial \tau_2}{\partial \omega} - \frac{\partial \tau_2}{\partial \sigma} \frac{\partial \tau_1}{\partial \omega} = \det \Delta(\omega) > 0,$$

then the region on the right of $\mathcal{T}_{j_1, j_2, n}^{\pm k}$ has two more characteristic roots with positive real parts. If $\delta(\omega) < 0$, then the left region of $\mathcal{T}_{j_1, j_2, n}^{\pm k}$ has two more characteristic roots with

positive real parts. Since $\det \begin{pmatrix} R_0 & -I_0 \\ I_0 & R_0 \end{pmatrix} = R_0^2 + I_0^2 \geq 0$, we get that if $R_0^2 + I_0^2 \neq 0$, $\text{sign } \delta(\omega) = \text{sign}\{R_1 I_2 - R_2 I_1\}$. One can also verify that

$$R_1 I_2 - R_2 I_1 = \pm \omega^2 |P_2 \bar{P}_3 - P_0 \bar{P}_1| \sin(\psi_{1,n}).$$

Hence, $\text{sign } \delta(\omega \in \mathring{\Omega}_{k,n}) = \pm \text{sign}(\omega^2 |P_2 \bar{P}_3 - P_0 \bar{P}_1| \sin(\psi_{1,n}))$, where $\mathring{\Omega}_{k,n}$ denotes the interior of $\Omega_{k,n}$.

Lemma 3. *For any $k = 1, 2, \dots, r_n$, we have*

$$\delta(\omega \in \mathring{\Omega}_{k,n}) > 0 (< 0) \quad \forall [\tau_1(\omega), \tau_2(\omega)] \in \mathcal{T}_{j_1, j_2, n}^{+k} ([\tau_1(\omega), \tau_2(\omega)] \in \mathcal{T}_{j_1, j_2, n}^{-k}).$$

Therefore, the region on the right (left) of the crossing curve $\mathcal{T}_{j_1, j_2, n}^{+k}$ ($\mathcal{T}_{j_1, j_2, n}^{-k}$) has two more characteristic roots with positive real parts.

2.3 Hopf and double Hopf bifurcation theorem

Now we introduce the Hopf bifurcation theorem [10] and conclude the double Hopf bifurcation theorem.

Theorem 2. *For any $j = 1, 2, \dots, r_n$, \mathcal{T}_n^j is a Hopf bifurcation curve in the following sense: for any $p \in \mathcal{T}_n^j$ and for any smooth curve Γ intersecting with \mathcal{T}_n^j transversely at p , we define the tangent of Γ at p by \vec{l} . If $\partial \text{Re } \lambda / \partial \vec{l}|_p \neq 0$ and the other eigenvalues of (3) at p have nonzero real parts, then system (1) undergoes a Hopf bifurcation at p when parameters (τ_1, τ_2) cross \mathcal{T}_n^j at p along Γ .*

If there exist ω_{j_1, k_1} and ω_{j_2, k_2} such that $\mathcal{T}_{k_1}^{j_1}$ and $\mathcal{T}_{k_2}^{j_2}$ intersect, then there are two pairs of pure imaginary roots of (3) at the intersection. Thus, system (1) may undergoes double Hopf bifurcation at this intersection under certain conditions. Here we summarize the following double Hopf bifurcation theorem.

Theorem 3. *If two Hopf bifurcation curves $\mathcal{T}_{k_1}^{j_1}$ and $\mathcal{T}_{k_2}^{j_2}$ intersect at q , we define the tangent of $\mathcal{T}_{k_1}^{j_1}$ and $\mathcal{T}_{k_2}^{j_2}$ at q by \vec{l}_1 and \vec{l}_2 , respectively. In addition, if \vec{l}_1 and \vec{l}_2 are linearly independent, namely, for $\alpha_1, \alpha_2 \in \mathbb{R}$, $\alpha_1 \vec{l}_1 + \alpha_2 \vec{l}_2 = 0$ can only arrive at $\alpha_1 = \alpha_2 = 0$, then system (1) undergoes a double Hopf bifurcation at q .*

Now we can summarize the following theorem about the stability of E_* .

Theorem 4. *Assume that (H0) and (H1) are true. For any point $\tilde{P}(\bar{\tau}_1, \bar{\tau}_2)$ on the τ_1, τ_2 -plane, if there exists a curve segment \vec{l} connecting \tilde{P} and the origin such that \vec{l} does not intersect any stability switching curves, then E_* is stable when $\tau_1 = \bar{\tau}_1, \tau_2 = \bar{\tau}_2$.*

This theorem can be easily proved with the aid of Lemma 1. For a better understanding of this theorem, please refer to Fig. 7(a).

3 Normal form of double Hopf bifurcation

From Section 2 we get that system (1) may undergo double Hopf bifurcations near $E_*(u_*, v_*)$. To investigate the dynamics near the double Hopf singularity, we will calculate the normal forms on the center manifold near the double Hopf singularity by the method derived in [9].

Assume that $\tau_2 > \tau_1$, let $\bar{u}(x, t) = u(x, \tau_2 t) - u_*$, $\bar{v}(x, t) = v(x, \tau_2 t) - v_*$ and drop the bars. System (1) can be written as

$$\begin{aligned} \frac{\partial}{\partial t} \begin{pmatrix} u(x, t) \\ v(x, t) \end{pmatrix} &= \tau_2(D\Delta + A) \begin{pmatrix} u(x, t) \\ v(x, t) \end{pmatrix} + \tau_2 B \begin{pmatrix} u(x, t - \frac{\tau_1}{\tau_2}) \\ v(x, t - \frac{\tau_1}{\tau_2}) \end{pmatrix} \\ &+ \tau_2 C \begin{pmatrix} u(x, t - 1) \\ v(x, t - 1) \end{pmatrix} + \tau_2 \begin{pmatrix} f_1 \\ f_2 \end{pmatrix}, \end{aligned} \tag{12}$$

where

$$\begin{aligned} f_1 &= f_{11}u^2(x, t) + f_{12}u(x, t)v(x, t) + f_{13}u(x, t)u\left(x, t - \frac{\tau_1}{\tau_2}\right) \\ &+ f_{14}u^2(x, t)u\left(x, t - \frac{\tau_1}{\tau_2}\right) + f_{15}u^2(x, t)v(x, t) + f_{16}u^3(x, t) + O(4), \\ f_2 &= f_{21}u^2(x, t - 1) + f_{22}u(x, t - 1)v(x, t) + f_{23}u^3(x, t - 1) \\ &+ f_{24}u^2(x, t - 1)v(x, t) + O(4), \end{aligned}$$

and

$$\begin{aligned} f_{11} &= r\left(1 - \frac{u_*}{K}\right) + \frac{mbv_*}{(b + u_*)^3}, & f_{12} &= -\frac{mb}{(b + u_*)^2}, & f_{13} &= -\frac{r(2u_* - c)}{K}, \\ f_{14} &= -\frac{r}{K}, & f_{15} &= \frac{mb}{(b + u_*)^3}, & f_{16} &= -\frac{mbv_*}{(b + u_*)^4}, \\ f_{21} &= -\frac{mbv_*}{(b + u_*)^3}, & f_{22} &= \frac{mb}{(b + u_*)^2}, & f_{23} &= \frac{mbv_*}{(b + u_*)^4}, & f_{24} &= -\frac{mb}{(b + u_*)^3}. \end{aligned}$$

Define the real-valued Hilbert space

$$X = \left\{ (u, v)^T \in H^2(0, l\pi) \times H^2(0, l\pi), \frac{\partial u}{\partial x} = \frac{\partial v}{\partial x} = 0 \text{ at } x = 0, l\pi \right\}$$

and the complexification space of X by $X_{\mathbb{C}} := X \oplus iX = \{U_1 + iU_2, U_1, U_2 \in X\}$ with the general complex-value L^2 inner product $\langle U, V \rangle = \int_0^{l\pi} (\bar{u}_1 v_1 + \bar{u}_2 v_2) dx$ for $U = (u_1, u_2)^T, V = (v_1, v_2)^T \in X_{\mathbb{C}}$. Let $\mathcal{C} := C([-1, 0], X_{\mathbb{C}})$ denote the phase space with the sup norm. We write $u^t(\theta) = u(t + \theta), -1 \leq \theta \leq 0$.

Denote the double Hopf singularity by (τ_1^*, τ_2^*) , introduce two parameters $\sigma = (\sigma_1, \sigma_2)$ with $\sigma_1 = \tau_1 - \tau_1^*$ and $\sigma_2 = \tau_2 - \tau_2^*$, denote $U(t) = [u(t), v(t)]^T$, then system (12) can be written as

$$\begin{aligned} \frac{dU(t)}{dt} &= D(\tau_1^* + \sigma_1, \tau_2^* + \sigma_2)\Delta U(t) + L(\tau_1^* + \sigma_1, \tau_2^* + \sigma_2)(U^t) \\ &+ F(\tau_1^* + \sigma_1, \tau_2^* + \sigma_2, U^t), \end{aligned} \tag{13}$$

where

$$\begin{aligned}
 D(\tau_1^* + \sigma_1, \tau_2^* + \sigma_2) &= \tau_2^* D + \sigma_2 D, \\
 L(\tau_1^* + \sigma_1, \tau_2^* + \sigma_2) &= (\tau_2^* + \sigma_2^*) \left(AU^t(0) + CU^t(-1) + BU^t \left(-\frac{\tau_1^*}{\tau_2^*} \right) \right) \\
 &\quad + (\tau_2^* + \sigma_2^*) \left(BU^t \left(-\frac{\tau_1^* + \sigma_1}{\tau_2^* + \sigma_2} \right) - BU^t \left(-\frac{\tau_1^*}{\tau_2^*} \right) \right).
 \end{aligned}$$

Linearizing system (13) at $(0, 0)$, we have

$$\begin{aligned}
 \frac{dU(t)}{dt} &= \tau_2^* \left[D\Delta U(t) + AU^t(0) + CU^t(-1) + BU^t \left(-\frac{\tau_1^*}{\tau_2^*} \right) \right] \\
 &\triangleq D_0\Delta U(t) + L_0(U^t),
 \end{aligned} \tag{14}$$

It is well known that the eigenvalues of $D\Delta$ on X are $-d_1 n^2/l^2$ and $-d_2 n^2/l^2$ with corresponding normalized eigenfunctions $\beta_n^{(1)}(x) = \gamma_n(x)(1, 0)^T$, $\beta_n^{(2)}(x) = \gamma_n(x)(0, 1)^T$ with $\gamma_n(x) = \cos((n/l)x)/\|\cos((n/l)x)\|_{L^2}$. Define the subspace of \mathcal{C} as \mathcal{B}_n , where \mathcal{B}_n is defined by $\mathcal{B}_n := \text{span}\{\langle v(\cdot), \beta_n^{(j)} \rangle \beta_n^{(j)}, v \in \mathcal{C}, j = 1, 2, \dots, n\}$. System (13) can be written as

$$\frac{dU(t)}{dt} = D_0\Delta U(t) + L_0(U^t) + G(\sigma, U^t), \tag{15}$$

where

$$\begin{aligned}
 G(\sigma, U^t) &= \sigma_2 \left[D\Delta U^t(0) + AU^t(0) + CU^t(-1) + BU^t \left(-\frac{\tau_1^*}{\tau_2^*} \right) \right] \\
 &\quad + (\tau_2^* + \sigma_2) B \left\{ U^t \left(-\frac{\tau_1^* + \sigma_1}{\tau_2^* + \sigma_2} \right) - U^t \left(-\frac{\tau_1^*}{\tau_2^*} \right) \right\} \\
 &\quad + F(\tau_1^* + \sigma_1, \tau_2^* + \sigma_2, U^t).
 \end{aligned}$$

Formulating (15) in the extended Banach space:

$$\mathcal{BC} := \left\{ \psi : [-1, 0] \rightarrow X_{\mathbb{C}}, \psi \text{ is continuous on } [-1, 0), \exists \lim_{\theta \rightarrow 0^-} \psi(\theta) \in X_{\mathbb{C}} \right\},$$

rewrite (15) as an abstract ordinary differential equations on \mathcal{BC} , then

$$\frac{d}{dt} U^t = \mathcal{A}U^t + X_0 G(\sigma, U^t), \tag{16}$$

where \mathcal{A} is the infinitesimal generator of the C_0 -semigroup of solution maps of the linear equation (14) defined by

$$\mathcal{A} : C_0^1 \cap \mathcal{BC} \rightarrow \mathcal{BC}, \quad \mathcal{A}\phi = \dot{\phi} + X_0 [D_0\Delta\phi(0) + L_0(\phi) - \dot{\phi}],$$

with $\text{dom}(\mathcal{A}) = \{\phi \in \mathcal{BC} : \dot{\phi} \in \mathcal{BC}, \phi(0) \in \text{dom}(\Delta)\}$ with $X_0(\theta) = 0$ for $\theta \in [-1, 0)$ and $X_0(0) = I$. On \mathcal{B}_n , system (14) is equivalent to the retarded functional differential equation

$$\dot{z}(t) = -\frac{k_m^2}{l^2} D_0 z(t) + L_0 z^t \tag{17}$$

on \mathbb{R}^2 . Thus, there exist matrix functions $\eta_m \in \text{BV}([-1, 0], \mathbb{R})$ such that $-(k_m^2/l^2) \times D_0\varphi(0) + L_0(\varphi) = \int_{-1}^0 d\eta_m(\theta)\varphi(\theta)$. Let \mathcal{A}_n denote the infinitesimal generator of the semigroup generated by (17), \mathcal{A}_n^* denote the formal adjoint of \mathcal{A}_n under the bilinear form

$$(\alpha, \beta)_m = \alpha(0)\beta(0) - \int_{-1}^0 \int_0^\theta \alpha(\xi - \theta) d\eta_m(\theta)\beta(\xi) d\xi.$$

System (14) has two pairs of pure imaginary eigenvalues $\pm i\omega_1\tau_2^*$ and $\pm i\omega_2\tau_2^*$ at the double Hopf singularity and the other eigenvalues with nonzero real parts. Here we do not consider the strongly resonant cases, i.e., $\omega_1 : \omega_2 \neq p : q$ for $p, q \in \mathbb{N}$ and $1 \leq p, q \leq 3$. Let $\phi_1(\theta) = (1, p_{12})^T e^{i\omega_1\tau_2^*\theta}$, $\phi_3(\theta) = (1, p_{32})^T e^{i\omega_2\tau_2^*\theta}$ ($\theta \in [-1, 0]$) are the eigenvectors of \mathcal{A}_m ($m = 1, 2$) corresponding to the eigenvalue $i\omega_1\tau_2^*$, $i\omega_2\tau_2^*$, respectively. Let $\psi_1(s) = D_1(1, p_{12}^*)e^{-i\omega_1\tau_2^*s}$, $\psi_3(s) = D_3(1, p_{32}^*)e^{-i\omega_2\tau_2^*s}$ ($s \in [0, 1]$) are the eigenvectors of \mathcal{A}_m^* ($m = 1, 2$) corresponding to the eigenvalue $i\omega_1\tau_2^*$, $i\omega_2\tau_2^*$, respectively. Choose Φ_m and Ψ_m^* as the basis of the generalized eigenspace of $\mathcal{A}_m, \mathcal{A}_m^*$ corresponding to the eigenvalues $\{\pm i\omega_1\tau_2^*, \pm i\omega_2\tau_2^*\}$, respectively, which

$$\begin{aligned} \Phi_1(\theta) &= (\phi_1(\theta), \phi_2(\theta)), & \Phi_2(\theta) &= (\phi_3(\theta), \phi_4(\theta)), & \Phi(\theta) &= (\Phi_1(\theta), \Phi_2(\theta)), \\ \Psi_1(s) &= (\psi_1(s), \psi_2(s))^T, & \Psi_2(s) &= (\psi_3(s), \psi_4(s))^T, & \Psi(s) &= (\Psi_1(s), \Psi_2(s))^T, \end{aligned}$$

with $\phi_2(\theta) = \overline{\phi_1(\theta)}$, $\phi_4(\theta) = \overline{\phi_3(\theta)}$, $\psi_2(s) = \overline{\psi_1(s)}$, $\psi_4(s) = \overline{\psi_3(s)}$ and satisfy $\mathcal{A}_m\Phi_m = \Phi_mB_{k_1}, \mathcal{A}_m^*\Psi_m = B_{k_2}\Psi_m, (\Psi_m, \Phi_m)_m = I$ with $B_{k_1} = \text{diag}(i\omega_1\tau_2^*, -i\omega_1\tau_2^*)$ and $B_{k_2} = \text{diag}(i\omega_2\tau_2^*, -i\omega_2\tau_2^*)$. By direct calculations, we get that

$$\begin{aligned} p_{12} &= \frac{c_{21}e^{-i\omega_1\tau_2^*}}{i\omega_1 + d_2 \frac{n^2}{l^2}}, & p_{12}^* &= \frac{-d}{i\omega_1 + d_2 \frac{n^2}{l^2}}, & p_{32} &= \frac{c_{21}e^{-i\omega_2\tau_2^*}}{i\omega_2 + d_2 \frac{n^2}{l^2}}, & p_{32}^* &= \frac{-d}{i\omega_2 + d_2 \frac{n^2}{l^2}}, \\ D_1 &= \frac{1}{1 + p_{12}^*p_{12} + \tau_2^*c_{21}p_{12}^*e^{-i\omega_1\tau_2^*} + \tau_1^*b_{11}e^{-i\omega_1\tau_1^*}}, \\ D_2 &= \frac{1}{1 + p_{32}^*p_{32} + \tau_2^*c_{21}p_{32}^*e^{-i\omega_2\tau_2^*} + \tau_1^*b_{11}e^{-i\omega_2\tau_1^*}}. \end{aligned}$$

Now decompose \mathcal{BC} into a direct sum of center subspace and its complementary space: $\mathcal{BC} = \mathcal{P} \oplus \text{Ker } \pi$, where $\pi : \mathcal{BC} \rightarrow \mathcal{P}$ is the projection defined by $\pi(\varphi) = \sum_{m=1}^2 \Phi_m(\Psi_m, \langle \varphi(\cdot), \beta_{k_m} \rangle)_m \cdot \beta_{k_m}$. Then we decompose $U^t(\theta) \in \mathcal{C}_0^1$ into $U^t(\theta) = \phi_1(\theta)z_1\gamma_{k_1} + \overline{\phi_1}(\theta)z_2\gamma_{k_1} + \phi_3(\theta)z_3\gamma_{k_2} + \overline{\phi_3}(\theta)z_4\gamma_{k_2} + w(\theta) \triangleq \Phi(\theta)z_x + w(\theta)$, where $w(\theta) \in \mathcal{C}_0^1 \cap \text{Ker } \pi := \mathcal{Q}^1$ for any t . Then in \mathcal{BC} , system (16) is equivalent to

$$\begin{aligned} \dot{z}_1 &= i\omega_1\tau_2^*z_1 + \psi_1(0)\langle G[\sigma, \Phi(\theta)z_x + w(\theta)], \beta_{k_1} \rangle, \\ \dot{z}_2 &= -i\omega_1\tau_2^*z_2 + \overline{\psi_1}(0)\langle G[\sigma, \Phi(\theta)z_x + w(\theta)], \beta_{k_1} \rangle, \\ \dot{z}_3 &= i\omega_2\tau_2^*z_3 + \psi_3(0)\langle G[\sigma, \Phi(\theta)z_x + w(\theta)], \beta_{k_2} \rangle, \\ \dot{z}_4 &= -i\omega_2\tau_2^*z_4 + \overline{\psi_3}(0)\langle G[\sigma, \Phi(\theta)z_x + w(\theta)], \beta_{k_2} \rangle, \\ \dot{w} &= \mathcal{A}^1w + (I - \pi)X_0G[\sigma, \Phi(\theta)z_x + w(\theta)], \end{aligned} \tag{18}$$

where \mathcal{A}^1 is the restriction of \mathcal{A} on $\mathcal{Q}^1 \subset \text{Ker } \pi \rightarrow \text{Ker } \pi$, $\mathcal{A}^1\phi = \mathcal{A}\phi$ for $\phi \in \mathcal{Q}^1$.

Consider the formal Taylor expansion $G(\sigma, \varphi) = \sum_{j=2}^{\infty} (1/j!)G_j(\sigma, \varphi)$, where G_j is the j th Fréchet derivation of G . Then we can rewrite (18) as

$$\dot{z} = Bz + \sum_{j=2}^{\infty} \frac{1}{j!} f_j^1(z, w, \sigma), \quad \dot{w} = \mathcal{A}^1 w + \sum_{j=2}^{\infty} \frac{1}{j!} f_j^2(z, w, \sigma), \quad (19)$$

where $z = (z_1, z_2, z_3, z_4)^T \in \mathbb{C}^4$, $w \in \mathcal{Q}^1$, and $f_j = (f_j^1, f_j^2)$, $j \geq 2$, are given by

$$f_j^1(z, w, \sigma) = \begin{pmatrix} \psi_1(0) \langle G_j(\sigma, \Phi(\theta)z_x + w(\theta)), \beta_{k_1} \rangle \\ \bar{\psi}_1(0) \langle G_j(\sigma, \Phi(\theta)z_x + w(\theta)), \beta_{k_1} \rangle \\ \psi_3(0) \langle G_j(\sigma, \Phi(\theta)z_x + w(\theta)), \beta_{k_2} \rangle \\ \bar{\psi}_3(0) \langle G_j(\sigma, \Phi(\theta)z_x + w(\theta)), \beta_{k_2} \rangle \end{pmatrix},$$

$$f_j^2(z, w, \sigma) = (\mathbf{I} - \pi)X_0 G_j[\sigma, \Phi(\theta)z_x + w(\theta)].$$

For a normed space Y , $V_j^{4+2}(Y)$ denotes the space of homogeneous polynomials of degree j in $z \in \mathbb{C}^4$, $\sigma = (\sigma_1, \sigma_2)$ with coefficients in Y , we have

$$V_j^{4+2}(Y) = \left\{ \sum_{|(q,l)|=j} c_{(q,l)} z^q \sigma^l, (q, l) \in \mathbb{N}_0^{4+2}, c_{(q,l)} \in Y \right\}$$

and the norm $|\sum_{|(q,l)|=j} c_{(q,l)} z^q \sigma^l| = \sum_{|(q,l)|=j} |c_{(q,l)}|_Y$. Define the operator $M_j = (M_j^1, M_j^2)$, $j \geq 2$, by

$$M_j^1 : V_j^{4+2}(\mathbb{C}^4) \rightarrow V_j^{4+2}(\mathbb{C}^4),$$

$$(M_j^1 p)(z, \sigma) = D_z p(z, \sigma) Bz - Bp(z, \sigma),$$

$$M_j^2 : V_j^{4+2}(\mathcal{Q}^1) \subset V_j^{4+2}(\text{Ker } \pi) \rightarrow V_j^{4+2}(\text{Ker } \pi),$$

$$(M_j^2 h)(z, \sigma) = D_z h(z, \sigma) Bz - \mathcal{A}^1 h(z, \sigma).$$

By a recursive transformations of variables $(z, w, \sigma) = (\hat{z}, \hat{w}, \sigma) + (1/j!)(U_j^1(\hat{z}, \sigma), U_j^2(\hat{z}, \sigma), 0)$ with $U_j = (U_j^1, U_j^2) \in V_j^{4+2}(\mathbb{C}^4) \times V_j^{4+2}(\mathcal{Q}^1)$, we can obtain the normal forms of (19). We conclude that this recursive process transforms (19) into the following equation:

$$\dot{z} = Bz + \sum_{j=2}^{\infty} \frac{1}{j!} g_j^1(z, w, \sigma), \quad \dot{w} = \mathcal{A}^1 w + \sum_{j=2}^{\infty} \frac{1}{j!} g_j^2(z, w, \sigma),$$

where $g_j = (g_j^1, g_j^2)$ have the following form $g_j(z, w, \sigma) = \bar{f}_j(z, w, \sigma) - M_j U_j(z, \sigma)$, and $U_j \in V_j^{4+2}(\mathbb{C}^4) \times V_j^{4+2}(\mathcal{Q}^1)$ satisfying $U_j(z, \sigma) = (M_j)^{-1} \text{Proj}_{\text{Im}(M_j^1) \times \text{Im}(M_j^2)} \circ \bar{f}_j(z, 0, \sigma)$, where $\bar{f}_j = (\bar{f}_j^1, \bar{f}_j^2)$ stand for the terms of order j in (z, w) , which are obtained after the computation of normal forms up to order $j - 1$. The normal form truncated to the third order has the form

$$\dot{z} = Bz + \frac{1}{2!} g_2^1(z, 0, \sigma) + \frac{1}{3!} g_3^1(z, 0, 0) + \text{h.o.t.}$$

Here, $g_3^1(z, 0, 0) = \text{Proj}_{\text{Ker}(M_3)} \bar{f}_3^1(z, 0, 0)$ and $\bar{f}_3^1(z, 0, 0) = f_3^1(z, 0, 0) + (3/2) \times [D_z f_2^1(z, 0, 0)U_2^1(z, 0)] + D_w f_2^1(z, 0, 0)U_2^1(Z, 0) - D_z U_2^1(z, 0)g_2^1(z, 0, 0)$. The calculations of $g_2^1(z, 0, \sigma)$ and $g_3^1(z, 0, 0)$ are the same as the calculation in [10]. After the calculations, the normal form truncated to the third order on the center manifold for double Hopf bifurcation can be obtained. By making the polar coordinate transformation

$$\begin{aligned} z_1 &= \rho_1 \cos \theta_1 + i\rho_1 \sin \theta_1, & z_2 &= \rho_1 \cos \theta_1 - i\rho_1 \sin \theta_1, \\ z_3 &= \rho_2 \cos \theta_2 + i\rho_2 \sin \theta_2, & z_4 &= \rho_2 \cos \theta_2 - i\rho_2 \sin \theta_2, \end{aligned}$$

where $\rho_1, \rho_2 > 0$. Take $\hat{\rho}_1 = \rho_1 \sqrt{|K_{2100}|}$, $\hat{\rho}_2 = \rho_2 \sqrt{|K_{0021}|}$, $\epsilon_1 = \text{sign}(\text{Re } K_{2100})$, $\epsilon_2 = \text{sign}(\text{Re } K_{0021})$, $\hat{t} = t\epsilon_1$ and drop the hats. We obtain the simplified system

$$\dot{\rho}_1 = \rho_1(v_1 + \rho_1^2 + b_0\rho_2^2), \quad \dot{\rho}_2 = \rho_2(v_2 + c_0\rho_1^2 + d_0\rho_2^2), \tag{20}$$

where $v_1 = \epsilon_1(\text{Re } K_{11}\sigma_1 + \text{Re } K_{21}\sigma_2)$, $v_2 = \epsilon_1(\text{Re } K_{13}\sigma_1 + \text{Re } K_{23}\sigma_2)$, $b_0 = \epsilon_1\epsilon_2 \times \text{Re } K_{1011} / \text{Re } K_{0021}$, $c_0 = \text{Re } K_{1110} / \text{Re } K_{2100}$ and $d_0 = \epsilon_1\epsilon_2$.

As was discussed in [12, Chap. 7.5], there are 12 distinct kinds of unfoldings for (20). In Section 4.1, three cases arise, thus we will draw the bifurcation sets and phase portraits for the unfoldings of case VIII and VIb for illustration.

4 Numerical simulations

In this section, we will do some numerical simulations to check the previous theoretical results. Besides, we will qualitatively analyze the influence of the small perturbations of c and K on the existence of the double Hopf bifurcations.

Now we carry out some simulations for system (1). Choose

$$\begin{aligned} r &= 1.2, & K &= 3, & m &= 1.8, & b &= 2, & c &= 1, \\ d &= 1, & d_1 &= 1, & d_2 &= 1, & l &= 3. \end{aligned} \tag{21}$$

One can verify that (H0) holds and E_* is (2.5, 0.75). Since $a_{11} + b_{11} = -0.8333 < 0$, (H1) holds, and E_* is locally stable for $\tau_1 = \tau_2 = 0$.

When τ_1, τ_2 vary simultaneously, we follow the process presented in Section 2.1. As is shown in Fig. 1(a), $F_0(0) > 0$ and $F_0(\omega) = 0$ has four zeros $a_{1,0} = 0.06146$, $b_{1,0} = 0.16390$, $a_{2,0} = 1.22056$, $b_{2,0} = 1.44592$, the crossing set is $\Omega_{1,0} \cup \Omega_{2,0} = [a_{1,0}, b_{1,0}] \cup [a_{2,0}, b_{2,0}]$. For the two ends of $\Omega_{1,0}$, we have $\psi_{1,0}(a_{1,0}) = \pi$, $\psi_{2,0}(a_{1,0}) = 0$, $\psi_{1,0}(b_{1,0}) = 0$, and $\psi_{2,0}(b_{1,0}) = \pi$, thus $\delta_1^a = 1$, $\delta_1^b = 0$, $\delta_2^a = 0$, $\delta_2^b = 1$. From Eq. (11) we get that $\mathcal{T}_{0,j_1,j_2}^+$ connect $\mathcal{T}_{0,j_1+1,j_2}^-$ at the left point $a_{1,0}$ and $\mathcal{T}_{0,j_1,j_2-1}^-$ at the right point $b_{1,0}$. As to $\Omega_{2,0}$, we get $\psi_{1,0}(a_{2,0}) = 0$, $\psi_{2,0}(a_{2,0}) = \pi$, $\psi_{1,0}(b_{2,0}) = 0$, and $\psi_{2,0}(b_{2,0}) = 0$, thus $\delta_1^a = 0$, $\delta_1^b = 1$, $\delta_2^a = 0$, $\delta_2^b = 0$. From (11) we get that $\mathcal{T}_{0,j_1,j_2}^+$ connect $\mathcal{T}_{0,j_1,j_2-1}^-$ at $a_{2,0}$ and $\mathcal{T}_{0,j_1,j_2}^-$ at $b_{2,0}$. From Lemma 2 we obtain all the stability switching curves of $n = 0$ given by \mathcal{T}_0^1 and \mathcal{T}_0^2 , which are showed in Figs. 1(b) and (c), respectively. To give a clearer description of the stability crossing curves, we take the

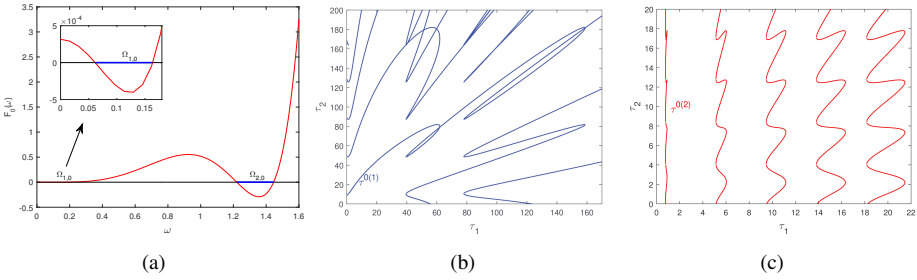


Figure 1. (a) Graph of $F_0(\omega)$. (b) Stability switching curves \mathcal{T}_0^1 . (c) Stability switching curves \mathcal{T}_0^2 .

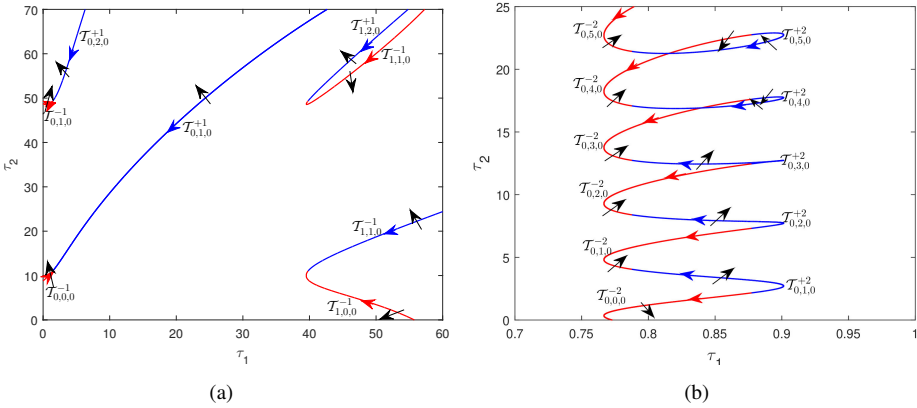


Figure 2. (a) The detailed structure of the lower left portion of \mathcal{T}_0^1 . (b) The detailed structure of the left-most curve of \mathcal{T}_0^2 . The blue (red) arrow represents the positive direction of $\mathcal{T}_{j_1, j_2, 0}^{+k}$ or $\mathcal{T}_{j_1, j_2, 0}^{-k}$.

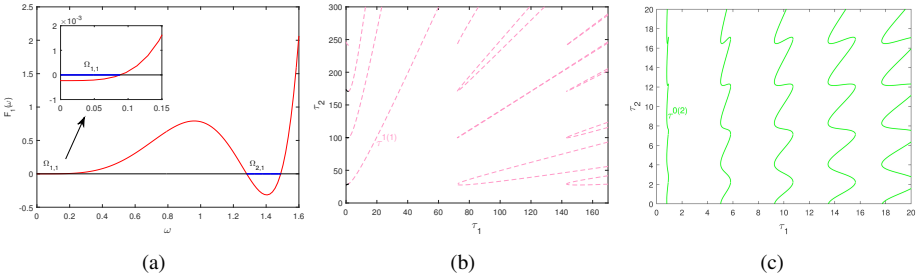


Figure 3. (a) Graph of $F_1(\omega)$. (b) Stability switching curves \mathcal{T}_1^1 . (c) Stability switching curves \mathcal{T}_1^2 .

lower left portion of \mathcal{T}_0^1 and the left-most curve of \mathcal{T}_0^2 as examples and draw the detailed figures in Fig. 2. The numerical results in Fig. 2 coincide with the theoretical analysis.

When $n = 1$, $F_1(\omega) = 0$ has three zeros $b_{1,1} = 0.08886$, $a_{2,1} = 1.28106$, $b_{2,1} = 1.48906$, and the crossing set is $\Omega_{1,1} \cup \Omega_{2,1} = [0, b_{1,1}] \cup [a_{2,1}, b_{2,1}]$. Then we get the stability switching curves \mathcal{T}_1^1 and \mathcal{T}_1^2 , which are shown in Figs. 3(b) and (c).

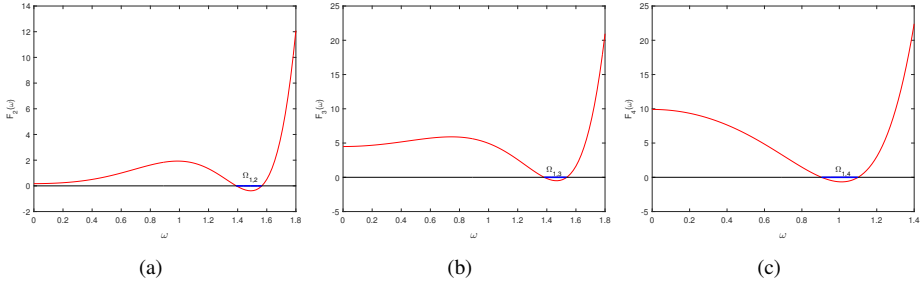


Figure 4. (a) Graph of $F_2(\omega)$. (b) Graph of $F_3(\omega)$. (c) Graph of $F_4(\omega)$.

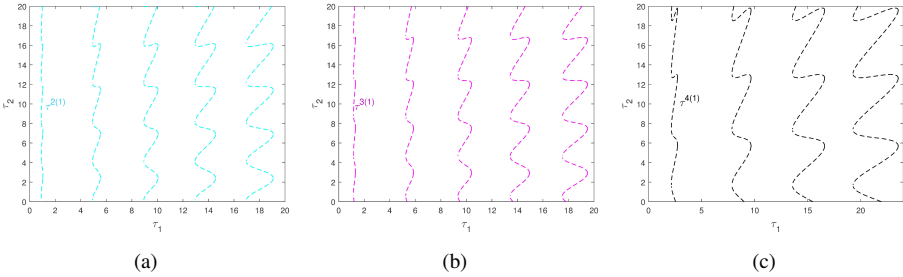


Figure 5. (a) Stability switching curves \mathcal{T}_2^1 . (b) Stability switching curves \mathcal{T}_3^1 . (c) Stability switching curves \mathcal{T}_4^1 .

When $n = 2$, $F_2(\omega) = 0$ has two zeros $a_{1,2} = 1.39120$, $b_{1,2} = 1.56591$, thus $\Omega_{1,2} = [a_{1,2}, b_{1,2}]$. The stability switching curves \mathcal{T}_2^1 are shown in Fig. 5(a). When $n = 3$, $F_3(\omega) = 0$ has two zeros $a_{1,3} = 1.3822$, $b_{1,3} = 1.5362$, thus $\Omega_{1,3} = [a_{1,3}, b_{1,3}]$, the stability switching curves \mathcal{T}_3^1 are shown in Fig. 5(b). When $n = 4$, $F_4(\omega) = 0$ has two zeros $a_{1,4} = 0.9052$, $b_{1,4} = 1.1001$, thus $\Omega_{1,4} = [a_{1,4}, b_{1,4}]$, the stability switching curves \mathcal{T}_4^1 are shown in Fig. 5(c). When $n \geq 5$, $F_n(\omega) > 0$ for all $\omega \geq 0$, thus there are no stability switching curves on the τ_1, τ_2 -plane.

Combining the stability switching curves shown in Figs. 1, 3, and 5 together, zooming them in one figure in $[0, 1.3] \times [0, 14]$, we get the stability switching curves shown in Fig. 6. By Lemma 2, we have plotted all the stability switching curves in $[0, 1.3] \times [0, 14]$.

We focus on the lower bottom region bounded by left-most curve of \mathcal{T}_0^1 , \mathcal{T}_1^1 and the lowest curve of \mathcal{T}_0^2 in Fig. 6. By Lemma 1, E_* is stable in the bottom left region, since the crossing directions of the three stability switching curves are all pointing outside of this region. These three stability crossing curves intersect at $\text{HH}_1(0.7717, 9.8717)$, $\text{HH}_2(0.8413, 7.9598)$, and $\text{HH}_3(0.9011, 7.6982)$. By the normal form derivation process in Section 3, we obtain the parameters in Table 1. For HH_1 , we get that case VIII occurs [12]. Near the double Hopf singularity HH_1 , there are six different kinds of phase diagrams in six regions, which are shown in Fig. 7(a). The six regions are divided by l_1, \dots, l_4 with $l_1: \sigma_2 = 1.5379\sigma_1$, $l_2: \sigma_2 = 62.6720\sigma_1$, $l_3: \sigma_2 = 58.5472\sigma_1$ ($\sigma_1 \geq 0$), $l_4: \sigma_2 = -15.1454\sigma_1$ ($\sigma_1 \geq 0$). For HH_2 , we get that case VIIb occurs. There are also six different kinds of phase diagrams in six regions near the double Hopf bifurcation

Table 1. Parameter values at the double Hopf points.

Point	n_1	ω_1	n_2	ω_2	d_0	b_0	c_0	Type
HH ₁	0	0.1622	0	1.3639	-1	-6.7643	-72.9979	VIII
HH ₂	0	1.3999	1	1.4755	-1	0.0947	-7.5179	VIb
HH ₃	0	1.2480	1	1.3925	1	0.0521	4.1036	Ia

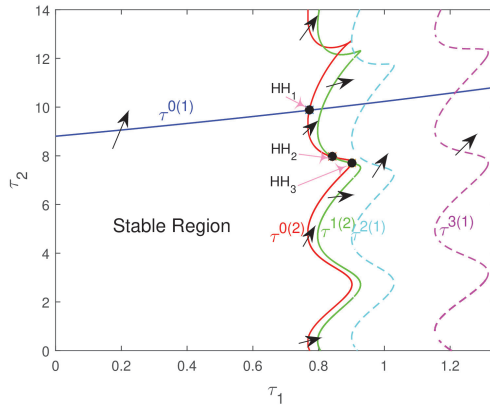


Figure 6. The stability switching curves and the intersections.

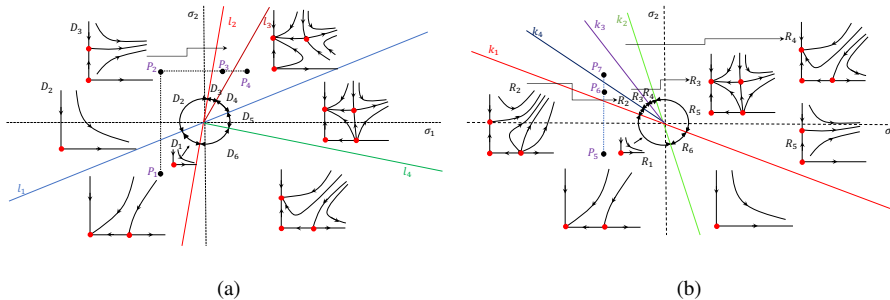


Figure 7. (a) Bifurcation diagram near HH₁. (b) Bifurcation diagram near HH₂.

point HH₂, which are shown in Fig. 7(b). The six regions are divided by k_1, \dots, k_4 with $k_1: \sigma_2 = -3.7480\sigma_1, k_2: \sigma_2 = -8.0660\sigma_1, k_3: \sigma_2 = -7.5157\sigma_1 (\sigma_1 \leq 0), k_4: \sigma_2 = -7.3311\sigma_1 (\sigma_1 \leq 0)$.

When (τ_1, τ_2) are chosen as $P_1(0.72, 9.7)$ in region D_1 , the positive equilibrium is a sink, which is shown in Fig. 8. When (τ_1, τ_2) are chosen as $P_2(0.775, 9.7)$ in D_2 or $P_3(0.775, 9.87)$ in D_3 , or $P_4(0.775, 9.7)$ in D_4 , there exists a stable periodic solution originating from the Hopf bifurcation. We only draw the case for $P_4 \in D_4$ in Fig. 9.

When $P_5(0.84, 7.95)$ falls in region R_1, E_* is a sink. When $P_6(0.84, 7.9662)$ is chosen in R_2 or $P_7(0.84, 7.9692)$ in R_3 , there exists a stable periodic solution. We only draw the case for $P_7 \in R_3$ in Fig. 10.

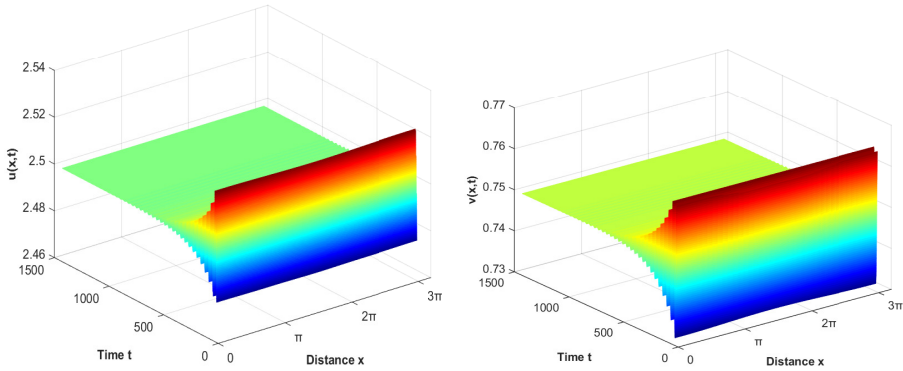


Figure 8. When $P_1 \in D_1$, the positive equilibrium is asymptotically stable, where the initial values are $u_0(x, t) = 2.55 + 0.5 \cos x$, $v_0(x, t) = 0.75 - 0.3 \cos x$.

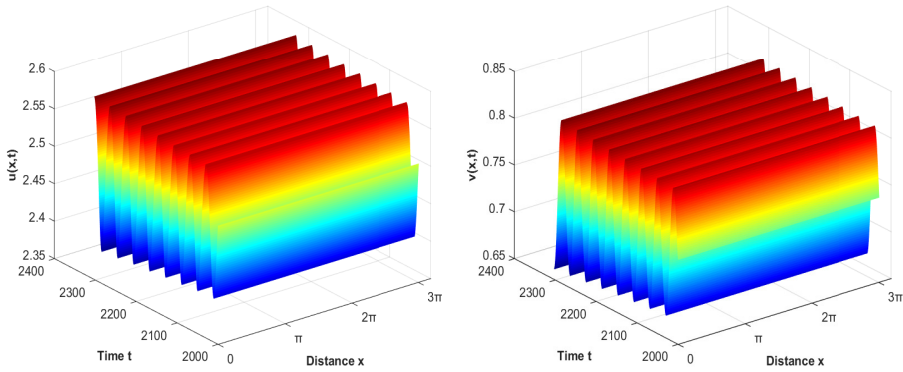


Figure 9. When $P_4 \in D_4$, the spatially homogeneous periodic solution is stable, where the initial values are $u_0(x, t) = 2.55 + 0.5 \cos x$, $v_0(x, t) = 0.75 - 0.3 \cos x$.

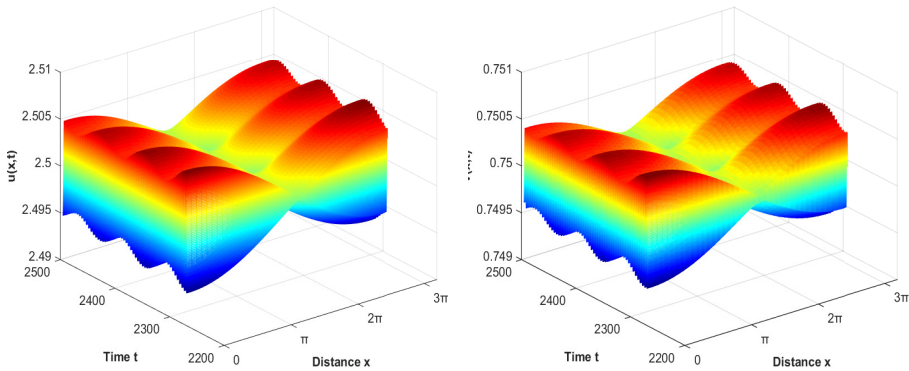


Figure 10. When $P_7 \in R_3$, the spatially inhomogeneous periodic solution is stable, where the initial values are $u_0(x, t) = 2.55 + 0.5 \cos x$, $v_0(x, t) = 0.75 - 0.3 \cos x$.

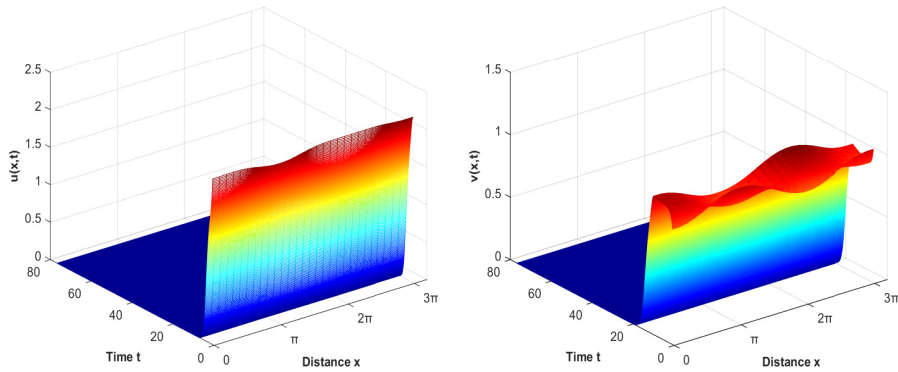


Figure 11. When $P_7 \in R_3$, $(0, 0)$ attracts the solution initiating from $u_0(x, t) = 2.55 + 0.5 \cos x$, $v_0(x, t) = 1 - 0.3 \cos x$.

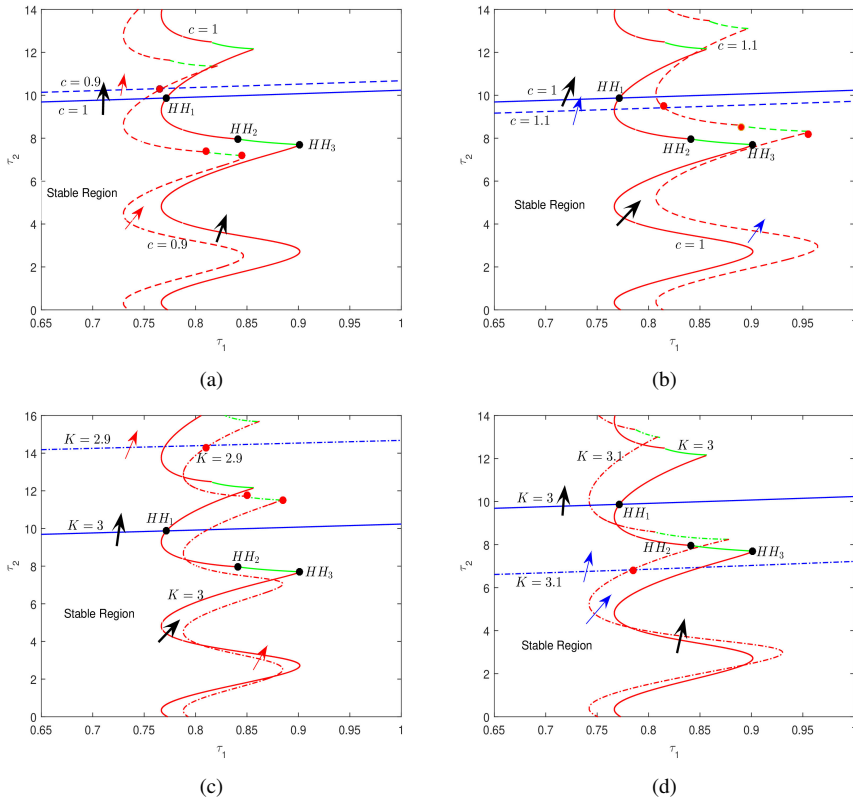


Figure 12. Stability switching curves with different parameters: (a) $c = 0.9$ and $c = 1$, drawn by dotted lines and solid lines, respectively; (b) $c = 1.1$ and $c = 1$, drawn by dotted lines and solid lines, respectively; (c) $K = 2.9$ and $K = 3$, drawn by dotted lines and solid lines, respectively; (d) $K = 3.1$ and $K = 3$, drawn by dotted lines and solid lines, respectively.

Since the strong Allee effect is considered in system (1), the over-predation phenomenon will occur when the initial value of the predator is large enough compared to the prey. We only take one example to show the over-predation phenomenon, which is revealed in Fig. 11.

Now we use parameters in (21) as a baseline to show the sensitivity of c and K on model (1) by numerical simulations.

First we consider the sensitivity of c on the stable region of E_* . We draw the left-most and bottom stability crossing curves and zoom them in $[0.65, 1] \times [0, 14]$ in Figs. 12(a) and (b). Then K is chosen as the perturbation parameter with all other parameters fixed as the same in (21). We also draw the left-most and bottom stability crossing curves and zoom them in $[0.65, 1] \times [0, 16]$ in Figs. 12(c) and (d).

From Fig. 12 we can conclude that although the influence of a slight perturbation of c or K on the stability region cannot be evaluated quantitatively, the double Hopf bifurcation still exist, which indicates that the double Hopf bifurcation in the system has strong anti-interference ability.

5 Conclusion

A diffusive predator–prey system with two delays and strong Allee effect is investigated in our paper. This system considers both the delay feedback of intraspecific competition in prey and the delay feedback of digestion in the predator. By applying the method of stability switching curves, we study the joint effect of the two delays on the stability of the positive constant steady state. With the aid of the crossing directions, we present the Hopf bifurcation theorem and give sufficient conditions for the existence of the double Hopf bifurcation.

To explore the dynamics of the system near the double Hopf singularities, we calculate the normal forms on the center manifold near the double Hopf singularities. The calculation formulas of the normal form we give here are at a double Hopf singularity with $k_1 = 0$, $k_2 = 1$. Then we get the corresponding unfoldings and the bifurcation sets. With a set of parameters, we theoretically prove and illustrate the existence of homogeneous and inhomogeneous periodic solution. Besides, heteroclinic orbits are found near the double Hopf singularity.

Populations with strong Allee effect can be wiped out by the over-predation phenomenon, we prove this phenomenon numerically. Finally, we carry out the sensitivity analysis to show the impact of two parameters on the dynamics of the system. Numerical simulation shows that small changes of c or K normally won't affect the existence of double Hopf singularities of the system.

Acknowledgment. The authors thank the two anonymous referees for their very helpful comments which greatly improve the manuscript.

References

1. W.C. Allee, E.S. Bowen, Studies in animal aggregations: Mass protection against colloidal silver among goldfishes, *J. Exp. Zool.*, **61**(2):185–207, 1932, <https://doi.org/10.1002/jez.1400610202>.
2. Q. An, E. Beretta, Y. Kuang, C. Wang, H. Wang, Geometric stability switch criteria in delay differential equations with two delays and delay dependent parameters, *J. Differ. Equations*, **266**(11):7073–7100, 2019, <https://doi.org/10.1016/j.jde.2018.11.025>.
3. E. Beretta, Y. Kuang, Convergence results in a well-known delayed predator–prey system, *J. Math. Anal. Appl.*, **204**(3):840–853, 1996, <https://doi.org/10.1006/jmaa.1996.0471>.
4. D.S. Boukal, L. Berec, Single-species models of the Allee effect: extinction boundaries, sex ratios and mate encounters, *J. Theor. Biol.*, **218**(3):375–394, 2002, <https://doi.org/10.1006/jtbi.2002.3084>.
5. X. Chang, J. Shi, J. Zhang, Dynamics of a scalar population model with delayed Allee effect, *Int. J. Bifurcation Chaos*, **28**(12):1850153, 2018, <https://doi.org/10.1142/S0218127418501535>.
6. S. Chen, J. Shi, J. Wei, The effect of delay on a diffusive predator–prey system with Holling type-II predator functional response, *Commun. Pure Appl. Anal.*, **12**(1):481–501, 2013, <https://doi.org/10.3934/cpaa.2013.12.481>.
7. K.L. Cooke, Z. Grossman, Discrete delays, distributed delay and stability switches, *J. Math. Anal. Appl.*, **86**(2):592–627, 1982, [https://doi.org/10.1016/0022-247X\(82\)90243-8](https://doi.org/10.1016/0022-247X(82)90243-8).
8. F. Courchamp, L. Berec, J. Gascoigne, *Allee Effect in Ecology and Conservation*, Oxford Univ. Press, 2008, <https://doi.org/10.1093/acprof:oso/9780198570301.001.0001>.
9. Y. Du, B. Niu, Y. Guo, J. Wei, Double Hopf bifurcation in delayed reaction–diffusion system, *J. Dyn. Differ. Equations*, **32**(1):313–358, 2020, <https://doi.org/10.1007/s10884-018-9725-4>.
10. Y. Du, B. Niu, J. Wei, Two delays induce Hopf bifurcation and double Hopf bifurcation in a diffusive Leslie–Gower predator–prey system, *Chaos*, **29**(1):013101, 2019, <https://doi.org/10.1063/1.5078814>.
11. K. Gu, S. Niculescu, J. Chen, On stability crossing curves for general systems with two delays, *J. Math. Anal. Appl.*, **311**:231–253, 2005, <https://doi.org/10.1016/j.jmaa.2005.02.034>.
12. J. Guckenheimer, P. Holmes, *Nonlinear Oscillations, Dynamical Systems, and Bifurcations of Vector Fields*, Springer, New York, 1983.
13. M. Jankovic, S. Petrovskii, Are time delay always destabilizing? Revisiting the role of time delays and the Allee effect, *Theor. Ecol.*, **7**(4):335–349, 2014, <https://doi.org/10.1007/s12080-014-0222-z>.
14. Y. Kuang, *Delay Differential Equations with Applications in Population Dynamics*, Academic Press, New York, 1993.
15. M.A. Lewis, S.V. Petrovskii, J.R. Potts, *The Mathematics Behind Biological Invasions*, Springer, Cham, 2016, <https://doi.org/10.1007/978-3-319-32043-4>.

16. X. Lin, H. Wang, Stability analysis of delay differential equations with two discrete delays, *Can. Appl. Math. Q.*, **20**(4):519–533, 2012.
17. J. Liu, X. Zhang, Stability and Hopf bifurcation of a delayed reaction–diffusion predator–prey model with anti-predator behaviour, *Nonlinear Anal. Model. Control*, **24**(3):387–406, 2019, <https://doi.org/10.15388/NA.2019.3.5>.
18. R. Pearl, L. Reed, On the rate of growth of the population of the United States since 1790 and its mathematical representation, *Proc. Natl. Acad. Sci. USA*, **6**(6):275–288, 1920, <https://doi.org/10.1073/pnas.6.6.275>.
19. P.A. Stephens, W.J. Sutherland, Consequences of the Allee effect for behaviour, ecology and conservation, *Trends Ecol. Evol.*, **14**(10):401–405, 1999, [https://doi.org/10.1016/S0169-5347\(99\)01684-5](https://doi.org/10.1016/S0169-5347(99)01684-5).
20. P. Turchin, *Complex Population Dynamics a Theoretical/Empirical Synthesis*, Princeton Univ. Press, Princeton, NJ, 2003.
21. J. Wei, S. Ruan, Stability and bifurcation in a neurall network model with two delays, *Physica D*, **130**(3–4):255–272, 1999, [https://doi.org/10.1016/S0167-2789\(99\)00009-3](https://doi.org/10.1016/S0167-2789(99)00009-3).
22. J. Wei Y. Song, Y. Peng, Bifurcations for a predator–prey system with two delays, *J. Math. Anal. Appl.*, **337**(1):466–479, 2008, <https://doi.org/10.1016/j.jmaa.2007.04.001>.
23. R. Yang, C. Zhang, Dynamics in a diffusive predator–prey system with a constant prey refuge and delay, *Nonlinear Anal., Real World Appl.*, **31**:1–22, 2016, <https://doi.org/10.1016/j.nonrwa.2016.01.005>.
24. H. Zhao, X. Zhang, X. Huang, Hopf bifurcation and spatial patterns of a delayed biological economic system with diffusion, *Appl. Math. Comput.*, **266**(1):462–480, 2015, <https://doi.org/10.1016/j.amc.2015.05.089>.